Editors' Suggestion | Featured in Physics

Quantum Spin Ice Dynamics in the Dipole-Octupole Pyrochlore Magnet $Ce_2Zr_2O_7$

J. Gaudet,[1,2,3] E. M. Smith,[1] J. Dudemaine,[4] J. Beare,[1] C. R. C. Buhariwalla,[1] N. P. Butch,[3] M. B. Stone,[5] A. I. Kolesnikov,[5] Guangyong Xu,[3] D. R. Yahne,[6] K. A. Ross,[6,7] C. A. Marjerrison,[8] J. D. Garrett,[8] G. M. Luke,[1,7] A. D. Bianchi,[4,9] and B. D. Gaulin[1,7,8]

[1]*Department of Physics and Astronomy, McMaster University, Hamilton, Ontario, L8S 4M1, Canada*
[2]*Institute for Quantum Matter and Department of Physics and Astronomy, Johns Hopkins University, Baltimore, Maryland 21218, USA*
[3]*Center for Neutron Research, National Institute of Standards and Technology, MS 6100 Gaithersburg, Maryland 20899, USA*
[4]*Département de Physique, Université de Montréal, 2900 Boulevard Édouard-Montpetit, Montréal, Quebec, H3T 1J4, Canada*
[5]*Neutron Scattering Division, Oak Ridge National Laboratory, Oak Ridge, Tennessee 37831, USA*
[6]*Department of Physics, Colorado State University, 200 West Lake Street, Fort Collins, Colorado 80523-1875, USA*
[7]*Canadian Institute for Advanced Research, 661 University Avenue, Toronto, Ontario, M5G 1M1, Canada*
[8]*Brockhouse Institute for Materials Research, McMaster University, Hamilton, Ontario, L8S 4M1, Canada*
[9]*Regroupement Québécois sur les Matériaux de Pointe (RQMP), Quebec, H3T 3J7, Canada*

(Received 28 November 2018; revised manuscript received 15 March 2019; published 7 May 2019)

Neutron scattering measurements on the pyrochlore magnet $Ce_2Zr_2O_7$ reveal an unusual crystal field splitting of its lowest $J = 5/2$ multiplet, such that its ground-state doublet is composed of $m_J = \pm 3/2$, giving these doublets a dipole-octupole (DO) character with local Ising anisotropy. Its magnetic susceptibility shows weak antiferromagnetic correlations with $\theta_{CW} = -0.4(2)$ K, leading to a naive expectation of an all-in, all-out ordered state at low temperatures. Instead, our low-energy inelastic neutron scattering measurements show a dynamic quantum spin ice state, with suppressed scattering near $|\mathbf{Q}| = 0$, and no long-range order at low temperatures. This is consistent with recent theory predicting symmetry-enriched U(1) quantum spin liquids for such DO doublets decorating the pyrochlore lattice. Finally, we show that disorder, especially oxidation of powder samples, is important in $Ce_2Zr_2O_7$ and could play an important role in the low-temperature behavior of this material.

DOI: 10.1103/PhysRevLett.122.187201

The rare-earth pyrochlore oxides $R_2B_2O_7$, where R^{3+} and B^{4+} consist generally of rare-earth and transition-metal ions, respectively, display a wealth of both exotic and conventional magnetic ground states. Their R^{3+} ions decorate a network of corner-sharing tetrahedra, one of the archetypes for geometrical frustration in three dimensions. Because of strong crystal electric field (CEF) effects, the nature of the magnetic interactions in such materials are strongly influenced by their single-ion physics [1–3]. A naive theoretical description of the magnetic interactions in rare-earth pyrochlores is generally performed by introducing an *ad hoc* effective single-ion term in addition to Heisenberg exchange interactions. For example, Heisenberg antiferromagnetism with an effective Ising anisotropy leads to nonfrustrated all-in, all-out (AIAO) magnetic order, as seen in several heavy rare-earth iridate pyrochlores [4,5] and illustrated in the insert of Fig. 1(a). Heisenberg ferromagnetism and an effective Ising anisotropy give rise to a classical spin ice ground state [6], as seen in $(Ho, Dy)_2Ti_2O_7$ [7,8] and illustrated as the two-in, two-out (2I2O) local structure in the inset of Fig. 1(a). However, the magnetic interactions should be projected into pseudospin operators acting solely on the low-energy CEF states [3,9–13]. This procedure has been applied, e.g., in the Yb^{3+} [11,14,15] and Er^{3+} [12,16–18] XY pyrochlores, where CEF effects give rise to effective $S = 1/2$ quantum degrees of freedom that interact via anisotropic exchange interactions.

More recently, it has been realized that the precise composition of the ground-state crystal field doublets in rare-earth pyrochlores is crucial in determining the form of the microscopic Hamiltonian, and in itself, diversifies the possibility of quantum magnetic states [3,19]. This has been appreciated for some time in the case of non-Kramers doublets, based on magnetic ions with an even number of electrons, such as the $4f^2$ configuration in Pr^{3+}. Only the local z component of the spin operators transforms as a dipole, with the transverse components transforming as quadrupoles [20–22]. This restricts the form of the effective spin Hamiltonian and can stabilize quadrupolar phases that are not present in the phase diagram for dipolar doublets [23,24]. For Kramers ions with an odd number of electrons, such as $4f^1$ in Ce^{3+}, $4f^3$ in Nd^{3+}, and $4f^5$ in Sm^{3+}, a crystal field ground-state doublet with dipole-octupole (DO) character can be realized where the local z and x components transform as a dipole, but the local y component transforms as an octupole [19,25–27]. After a rotation of the pseudospins about the y axis, the DO exchange Hamiltonian on the pyrochlore lattice can be reduced to an XYZ model with

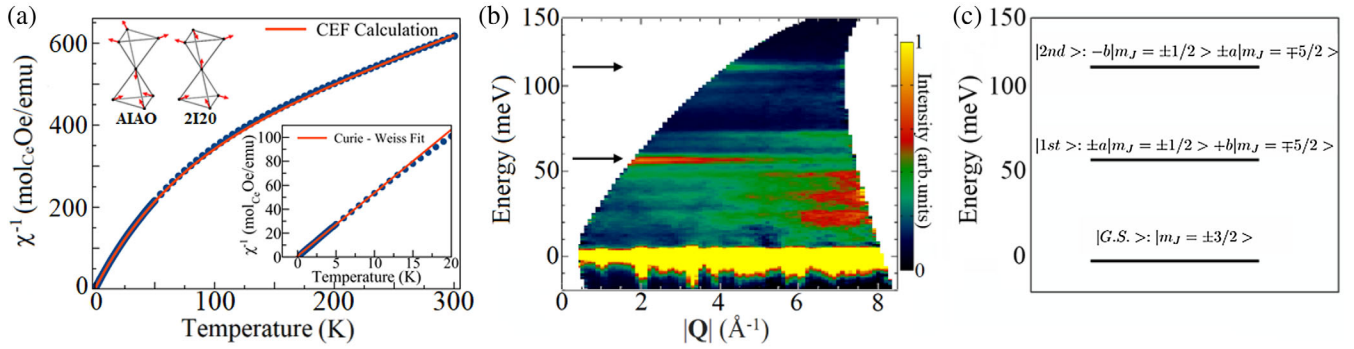

FIG. 1. (a) The inverse magnetic susceptibility of a powder sample of $Ce_2Zr_2O_7$. The red curve is the Van Vleck susceptibility calculated with the CEF Hamiltonian of $Ce_2Zr_2O_7$. (Top left inset) The AIAO and 2I2O magnetic ground-state spin configurations on a pair of tetrahedra. (Bottom right inset) The low-temperature magnetic susceptibility that yields $\theta_{CW} = -0.4(2)$ K and a paramagnetic moment of $1.3(1)$ μ_B and shows no signature of magnetic order or spin freezing down to 0.5 K. (b) Inelastic neutron scattering spectra of $Ce_2Zr_2O_7$ at $T = 5$ K with incident neutron energy $E_i = 150$ meV. Two strong excitations can be identified as magnetic in origin at $E \sim 56$ and ~ 112 meV, as their intensity decreases as a function of $|\mathbf{Q}|$, consistent with the Ce^{3+} magnetic form factor. (c) The energy eigenvalues corresponding to the CEF states belonging to the spin-orbit ground-state manifold of $Ce_2Zr_2O_7$. The composition of the CEF eigenfunctions are also presented in (c), revealing the DO nature of the ground-state doublet—that is, it corresponds to pure $m_J = \pm 3/2$ states.

three independent exchange parameters ($J_{\tilde{x}}$,$J_{\tilde{y}}$,$J_{\tilde{z}}$) [19,25]. This Hamiltonian allows for multiple phases to emerge, such as an AIAO order, octupolar ordered phases, and also for moment fragmentation, as observed in $Nd_2Zr_2O_7$, where static AIAO order coexists with dynamic spin ice fluctuations [19,25,28,29]. In the limit of dominant antiferromagnetic interactions and strong easy-axis exchange anisotropy, a dipolar quantum spin ice is stabilized so long as the easy axis is along one of the dipolar components of the DO doublet ($J_{\tilde{x}} \gg J_{\tilde{z}},J_{\tilde{y}}$ or $J_{\tilde{z}} \gg J_{\tilde{x}},J_{\tilde{y}}$). An octupolar quantum spin ice is favored if the easy axis is along the octupole component ($J_{\tilde{y}} \gg J_{\tilde{x}},J_{\tilde{z}}$) [19,25].

A promising family of candidate materials for dipolar or octupolar quantum spin ice physics originating from DO doublets are the cerium pyrochlores $Ce_2B_2O_7$. The Ce^{3+} ions in the pyrochlore $Ce_2Sn_2O_7$ are believed to have a DO CEF ground state and to interact via dominant antiferromagnetic interactions, but do not magnetically order down to $T = 20$ mK [25,30]. The low-energy spin dynamics of the cerium pyrochlores remains unexplored and their characterization is key in determining the nature of their possible spin liquid states. In this Letter, we report new inelastic neutron scattering experiments on powder and single crystal samples of $Ce_2Zr_2O_7$. Using high-energy inelastic neutron scattering, we first confirmed the DO nature of the Ce^{3+} single-ion ground-state wave functions in $Ce_2Zr_2O_7$. We also present low-energy inelastic neutron scattering measurements performed on a single crystal of $Ce_2Zr_2O_7$ and observe diffuse, inelastic magnetic scattering that emerges at low temperatures. The $\mathbf{Q}$ dependence of this diffuse scattering is consistent with a symmetry-enriched U(1) quantum spin ice state at low but finite temperatures. Furthermore, we show the quantum spin-ice correlations remain dynamic down to at least 60 mK with no sign of static magnetic order. Our results demonstrate $\mathbf{Q}$ signatures of a dynamic quantum spin ice ground state in $Ce_2Zr_2O_7$, with associated emergent quantum electrodynamics and elementary excitations based on magnetic and electric monopoles, as well as emergent photons [31–34].

Single crystal and powder samples of $Ce_2Zr_2O_7$ have been grown using floating zone techniques and solid-state synthesis. Stabilizing the Ce^{3+} oxidation state in $Ce_2Zr_2O_7$ is not simple and requires growth and annealing in strong reducing conditions to minimize Ce^{4+} [35]. As discussed in the Supplemental Material [36], which includes Refs. [37–44], this is a serious issue, especially in powder samples, where oxidization is observed to occur in powders exposed to air on a timescale on the order of minutes, complicating the exact characterization of the material's stoichiometry. The oxidization process can be tracked through high-resolution x-ray diffraction measurements of the lattice parameter, and it is much slower for single crystal samples. There we can make an estimate of the stoichiometry of the single crystal used in our experiments as $Ce_2Zr_2O_{7+\delta}$ with $\delta \sim 0.1$.

We first present high-energy inelastic neutron scattering measurements, which probe the single-ion properties of the Ce^{3+} ions. To do so, we used the SEQUOIA high-resolution inelastic chopper spectrometer [45] at the Spallation Neutron Source of Oak Ridge National Laboratory and employed neutrons with incident energies (E_i) of 150 and 500 meV. The $E_i = 150$ meV instrument setting was chosen to resolve the CEF states that belong to the spin-orbit ground-state manifold ($J = 5/2$). The CEF interaction lifts the Ce^{3+} spin-orbit ground-state degeneracy into three different eigenstates that are each doubly degenerate. We also estimated a CEF Hamiltonian for $Ce_2Zr_2O_7$ using a scaling procedure based on the Er^{3+} pyrochlore CEF

scheme [46]. This predicts two CEF excited states near 80 and 100 meV with similar inelastic neutron scattering intensity at $T = 5$ K. As seen in Fig. 1(b), this scenario is in qualitatively good agreement with our 150 meV inelastic neutron experimental spectra, where two strong magnetic excitations are observed at ~56 and ~112 meV. The relative scattered intensity of these CEF transitions can be obtained giving $I_{56\ \mathrm{meV}}/I_{112\ \mathrm{meV}} = 1.2(1)$, in good agreement with our expectations based on this scaling argument.

Additional weak inelastic scattering whose **Q** dependence is inconsistent with phonons is also visible in the spectra, e.g., weak scattering near ~100 meV in Fig. 1(b). It is not clear if this weak inelastic scattering is due to the influence of Ce^{3+} or Zr^{3+} in defective sites [47], on residual Ce^{4+}, or on the possible presence of hybridized phonon-crystal field excitations known as vibronic bound states, as has been recently observed in holmium and terbium pyrochlores [48,49]. In any case, this unidentified contribution to the inelastic scattering yields a small fraction of the spectral weight and we conclude the features at 56 and 112 meV are the CEF excitations corresponding to the main Ce^{3+} site.

The details of the crystal field analysis determining the full set of eigenvalues and eigenfunctions for Ce^{3+} are summarized in Fig. 1(c) and further discussed in the Supplemental Material [36]. The key conclusion is that the ground-state Kramers doublet appropriate to Ce^{3+} is well separated from all excited crystal field states (by ~56 meV) and is composed of pure $m_J = \pm 3/2$ states. A large CEF gap is consistent with the high-temperature heat capacity of $Ce_2Zr_2O_7$ measured in Ref. [50], where no Schottky anomaly is observed between 5 and 300 K. These pure $m_J = \pm 3/2$ states have a dipole-octupole character with a dipolar moment whose anisotropy is purely Ising and whose magnitude must be 1.286 μ_B. This result does not originate from a fine-tuning of the CEF parameters, but is instead a property protected by the point-group symmetry of the A site in the pyrochlore lattice.

Figure 1(a) shows the inverse magnetic susceptibility of a 107 mg powder sample of $Ce_2Zr_2O_7$ measured with a Quantum Design magnetic property measurement system magnetometer equipped with a ^{3}He insert. The main panel of Fig. 1(a) shows the high-temperature susceptibility of $Ce_2Zr_2O_7$ and reveals strong nonlinearity. Assuming a dilution of the Ce^{3+} moments by nonmagnetic Ce^{4+} ions at the ~8% level in this powder sample, the Van Vleck susceptibility calculated with the CEF Hamiltonian of $Ce_2Zr_2O_7$ reproduces the high-temperature susceptibility data well and yields an antiferromagnetic Curie constant of $-0.4(2)$ K. We expect conventional and unfrustrated AIAO order in $Ce_2Zr_2O_7$ based on the effective antiferromagnetic interactions and the Ising anisotropy associated with its magnetism. However, our magnetic susceptibility measurements [inset of Fig. 1(a)], as well as both powder and single crystal neutron diffraction experiments, show no indication of long-range magnetic order down to $T = 0.06$ K. In particular, and as shown in the Supplemental Material [36], no new Bragg scattering or enhancement of the Bragg scattering associated with any $\mathbf{k} = 0$ magnetic structure is observed, including at those wave vectors characteristic of the AIAO, Γ_3 structure. $Ce_2Zr_2O_7$ therefore remains disordered to $T = 0.06$ K, our lowest temperature measured.

We examined the low-temperature spin dynamics in $Ce_2Zr_2O_7$ using the low energy disk chopper spectrometer (DCS) neutron instrument at NCNR with $E_i = 3.27$ meV incident neutrons giving an energy resolution of ~0.09 meV at the elastic line. One experiment was performed on a ~6 g powder sample and a second one was performed on a ~5 g single crystal, which was mounted with its $[HHL]$ plane coincident with the horizontal plane of the spectrometer. Figure 2(a) shows the DCS measurements on our powder, where the integration in $|\mathbf{Q}|$ is $0.35 - 0.85$ Å^{-1}. This integration in momentum transfer $|\mathbf{Q}|$ corresponds to integrating over the $|\mathbf{Q}| = |(001)|$ position (~0.59 Å^{-1}), where quantum spin ice correlations are expected to be strongest [34]. A buildup of inelastic spectral weight below ~0.4 meV is observed on decreasing the temperature.

Low-energy inelastic neutron scattering from our single crystal is shown in Figs. 2(b)–2(d) and 3(a). All this data were acquired using the same $E_i = 3.27$ meV instrument configuration of DCS, and Figs. 2(b)–2(d) shows *powder-averaged* single crystal data. Figure 2(b) shows the full

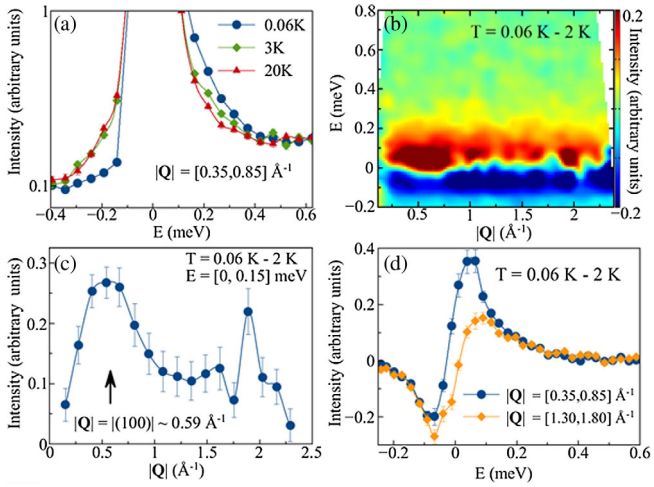

FIG. 2. (a) The onset of dynamic spin ice correlations with decreasing temperature in an annealed $Ce_2Zr_2O_7$ powder sample. (b) The powder-averaged *difference* neutron scattering spectra for an annealed single crystal sample of $Ce_2Zr_2O_7$. A dataset at $T = 2$ K has been subtracted from that at $T = 0.06$ K. (c) A cut along $|\mathbf{Q}|$ through this difference spectra showing that the dominant quasielastic signal, integrated in energy between 0 and 0.15 meV, is centered on $|\mathbf{Q}| = |(001)|$ (~0.59 Å^{-1}) and (d) a comparison of two cuts in energy through the difference spectra shown in (b), with one of these cuts taken with a $|\mathbf{Q}|$ integral centered on $|(001)|$ (0.35–0.85 Å^{-1}), and one removed from $|(001)|$, integrating between 1.3 and 1.8 Å^{-1}. For all these panels, the error bars correspond to 1 standard deviation.

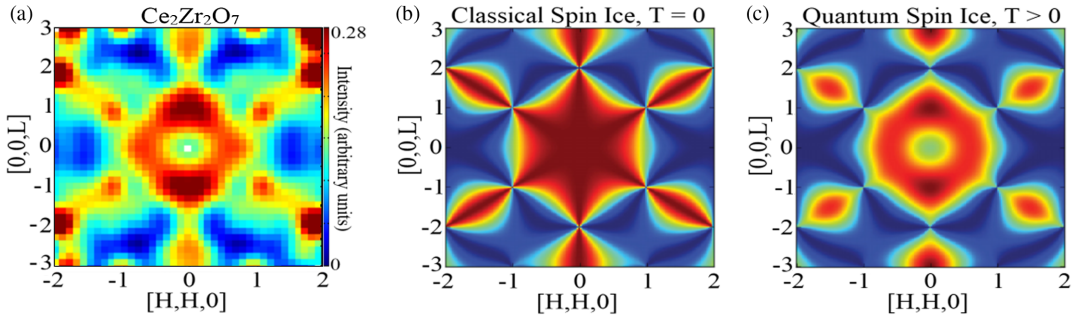

FIG. 3. Comparison of the measured low-energy inelastic neutron scattering from (a) an annealed single crystal sample of $Ce_2Zr_2O_7$ with the calculated quasielastic neutron scattering for (b) the classical near-neighbor spin ice model at $T = 0$ K and (c) a quantum spin ice at finite T. Data in (a) are the symmetrized difference between inelastic scattering at $T = 0.06$ K and $T = 2$ K, integrated between 0 and 0.15 meV. (b),(c) Simulations taken from Benton *et al.* [34]. The lack of intensity around $\mathbf{Q} = (000)$ and the fact that the ring of diffuse inelastic scattering peaks along $(00L)$ provides evidence for $Ce_2Zr_2O_7$ displaying a dynamic quantum spin ice state at these low temperatures. Also, the observed diffuse inelastic scattering at $\mathbf{Q} = (003)$ is more pronounced than that at $\mathbf{Q} = (\frac{3}{2}\frac{3}{2}\frac{3}{2})$, again consistent with the expectations of quantum spin ice, and not consistent with classical near-neighbor spin ice. Note the extra features centered at the Bragg peak positions such as (111) likely originate from leakages of the structural Bragg peaks, due to the subtraction of two large intensities.

powder-averaged spectrum at $T = 0.06$ K with a $T = 2$ K dataset subtracted from it. This result shows enhanced inelastic scattering at low temperature, which peaks up at $|\mathbf{Q}| \sim 0.59$ Å^{-1}, that is, the magnitude of the $\mathbf{Q} = (001)$ position in reciprocal space. This is explicitly shown via the $|\mathbf{Q}|$ cut of the data presented in Fig. 2(c). Importantly, Fig. 2(c) shows no enhancement of the low-energy inelastic scattering around $|\mathbf{Q}| = 0$, consistent with expectations for a U(1) quantum spin ice. Finally, Fig. 2(d) shows energy cuts through the full difference spectrum shown in Fig. 2(b), taken by integrating in $|\mathbf{Q}|$ from 0.35 to 0.85 Å^{-1}, so around $|\mathbf{Q}| = |(001)|$, and also well away from $|\mathbf{Q}| = |(001)|$, integrating from 1.3 to 1.8 Å^{-1}. This clearly shows the quantum spin ice correlations to be dynamic in nature, characterized by an energy less than ~0.15 meV.

With the energy range of the dynamic quantum spin ice correlations identified, we can look explicitly at this scattering from the single crystal, but now comparing $\mathbf{Q}$ maps of these correlations to the expectations of both classical near-neighbor spin ice (without dipolar interactions) and a U(1) quantum spin ice. Figure 3(a) shows $T = 0.06$–2 K data integrated between 0 and 0.15 meV, folded into a single quadrant of the $[HHL]$ map and further symmetrized. The details of this data symmetrization are in the Supplemental Material [36]. For reference, a theoretical simulation of the structure factor expected for classical near-neighbor spin ice [34] is shown in Fig. 3(b) and that for a U(1) quantum spin ice at low but finite temperature [34] is shown in Fig. 3(c). While these theoretical predictions have similarities, the structure factor for U(1) quantum spin ice has minima in intensity near $\mathbf{Q} = 0$, while the intensity of the structure factor is maximal there for classical near-neighbor spin ice.

Clearly, the measured dynamic $S(\mathbf{Q})$ shows a qualitatively stronger resemblance to the expectations of the symmetry-enriched U(1) quantum spin ice [31–34]. The quantum spin ice ground state is one of various spin liquids that are supported by a model of well isolated DO CEF doublets on the pyrochlore lattice [19,25]. A similar dynamic $S(\mathbf{Q})$ is expected in the case of classical *dipolar* spin ice (here dipolar refers to long-range dipolar interactions between magnetic dipoles), which also shows the suppression of diffuse scattering near $|\mathbf{Q}| = 0$ [51,52]. Although a definitive conclusion can only be reached once a full spin Hamiltonian is parametrized, the Ce^{3+} ions in $Ce_2Zr_2O_7$ have a moment of 1.286 μ_B, which is roughly a factor 8 smaller than those associated with Ho^{3+} or Dy^{3+} in the classical dipolar spin ices $Ho_2Ti_2O_7$ and $Dy_2Ti_2O_7$. The resulting long-range dipole terms are expected to be ~64 times weaker in $Ce_2Zr_2O_7$, making such a scenario unlikely. This suggests the spin-ice correlations in $Ce_2Zr_2O_7$ originate from quantum effects. An octupolar ordered state is also consistent with the lack of magnetic dipole order in $Ce_2Zr_2O_7$. However, the neutron scattering spectra associated with such an octupolar ordered phase has yet to be calculated; thus we cannot compare it to our data in Fig. 3(a).

The effect of disorder in $Ce_2Zr_2O_7$ is still an open question as we are aware that our single crystals have some low levels of oxidation. Furthermore, stuffing [53–56] (site mixing) is expected to be important in $Ce_2Zr_2O_7$, because both undesired Ce^{4+} and Zr^{3+} ions are chemically stable. It is known that small amounts of disorder can have a drastic impact on the physical properties of frustrated pyrochlore magnets [53,54,56]. It will then be important to further optimize the growth procedure and annealing techniques of $Ce_2Zr_2O_7$. However, we believe that our inelastic neutron scattering results rule out the scenario of a sensitive AIAO order. Indeed, the conventional impact of quenched disorder on a pyrochlore antiferromagnet would be spin glass physics with diffuse scattering peaked for $\mathbf{Q}$'s corresponding to the Bragg

positions of the AIAO state. Here, we observe strong diffuse scattering at $\mathbf{Q} = (001)$, which is not only strictly zero for an AIAO state, but also forbidden for all $\mathbf{k} = 0$ long-range ordered magnetic structures allowed by symmetry of the pyrochlore lattice. We thus conclude that our Letter demonstrates $Ce_2Zr_2O_7$ to be one of a very few candidates for quantum spin ice physics. Other candidates for quantum spin ice physics are based on Pr^{3+} and Tb^{3+} pyrochlores [57–61]. However, in contrast to Pr^{3+} and Tb^{3+}, Ce^{3+} is a Kramers ion and its magnetism is thus further protected against disorder, which in and of itself can drive a spin liquid state for non-Kramers doublets [22,62–64]. Furthermore, Tb^{3+} and Pr^{3+} pyrochlores display low-lying CEF field states, which complicate their theoretical understanding due to multipolar interactions [24,65,66]. For all these reasons, the cerium pyrochlores are an excellent theoretical and experimental template to investigate quantum spin ice physics.

We acknowledge useful conversations with Allen Scheie, Alannah Hallas, and Owen Benton. We greatly appreciate the technical support from Alan Ye and Yegor Vekhov at the NIST Center for Neutron Research. This work was supported by the Natural Sciences and Engineering Research Council of Canada (NSERC). A portion of this research used resources at the High Flux Isotope Reactor and Spallation Neutron Source, a DOE Office of Science User Facility operated by the Oak Ridge National Laboratory. We also acknowledge the support of the National Institute of Standards and Technology, U.S. Department of Commerce. Certain commercial equipment, instruments, or materials (or suppliers, or software, etc.) are identified in this Letter to foster understanding. Such identification does not imply recommendation or endorsement by the National Institute of Standards and Technology, nor does it imply that the materials or equipment identified are necessarily the best available for the purpose.

Note added in the proof.—Recently, we became aware of Ref. [67], which reports on a related experimental study on $Ce_2Zr_2O_7$.

[1] J. S. Gardner, M. J. P. Gingras, and J. E. Greedan, Rev. Mod. Phys. **82**, 53 (2010).
[2] A. M. Hallas, J. Gaudet, and B. D. Gaulin, Annu. Rev. Condens. Matter Phys. **9**, 105 (2018).
[3] J. G. Rau and M. J. P. Gingras, Annu. Rev. Condens. Matter Phys. **10**, 357 (2018).
[4] H. Sagayama, D. Uematsu, T. Arima, K. Sugimoto, J. J. Ishikawa, E. O'Farrell, and S. Nakatsuji, Phys. Rev. B **87**, 100403(R) (2013).
[5] S. M. Disseler, Phys. Rev. B **89**, 140413(R) (2014).
[6] S. T. Bramwell and M. J. P. Gingras, Science **294**, 1495 (2001).
[7] M. J. Harris, S. T. Bramwell, D. F. McMorrow, T. H. Zeiske, and K. W. Godfrey, Phys. Rev. Lett. **79**, 2554 (1997).
[8] D. J. P. Morris, D. A. Tennant, S. A. Grigera, B. Klemke, C. Castelnovo, R. Moessner, C. Czternasty, M. Meissner, K. C. Rule, J.-U. Hoffmann, K. Kiefer, S. Gerischer, D. Slobinsky, and R. S. Perry, Science **326**, 411 (2009).
[9] S. H. Curnoe, Phys. Rev. B **78**, 094418 (2008).
[10] S. Onoda, J. Phys. Conf. Ser. **320**, 012065 (2011).
[11] K. A. Ross, L. Savary, B. D. Gaulin, and L. Balents, Phys. Rev. X **1**, 021002 (2011).
[12] L. Savary, K. A. Ross, B. D. Gaulin, J. P. C. Ruff, and L. Balents, Phys. Rev. Lett. **109**, 167201 (2012).
[13] J. G. Rau and M. J. P. Gingras, Phys. Rev. B **92**, 144417 (2015).
[14] J. Robert, E. Lhotel, G. Remenyi, S. Sahling, I. Mirebeau, C. Decorse, B. Canals, and S. Petit, Phys. Rev. B **92**, 064425 (2015).
[15] J. D. Thompson, P. A. McClarty, D. Prabhakaran, I. Cabrera, T. Guidi, and R. Coldea, Phys. Rev. Lett. **119**, 057203 (2017).
[16] S. Petit, J. Robert, S. Guitteny, P. Bonville, C. Decorse, J. Ollivier, H. Mutka, M. J. P. Gingras, and I. Mirebeau, Phys. Rev. B **90**, 060410(R) (2014).
[17] A. M. Hallas, J. Gaudet, N. P. Butch, G. Xu, M. Tachibana, C. R. Wiebe, G. M. Luke, and B. D. Gaulin, Phys. Rev. Lett. **119**, 187201 (2017).
[18] S. Petit, E. Lhotel, F. Damay, P. Boutrouille, A. Forget, and D. Colson, Phys. Rev. Lett. **119**, 187202 (2017).
[19] Y.-P. Huang, G. Chen, and M. Hermele, Phys. Rev. Lett. **112**, 167203 (2014).
[20] S. B. Lee, S. Onoda, and L. Balents, Phys. Rev. B **86**, 104412 (2012).
[21] G. Chen, Phys. Rev. B **96**, 085136 (2017).
[22] N. Martin, P. Bonville, E. Lhotel, S. Guitteny, A. Wildes, C. Decorse, M. Ciomaga Hatnean, G. Balakrishnan, I. Mirebeau, and S. Petit, Phys. Rev. X **7**, 041028 (2017).
[23] S. Onoda and Y. Tanaka, Phys. Rev. B **83**, 094411 (2011).
[24] H. Takatsu, S. Onoda, S. Kittaka, A. Kasahara, Y. Kono, T. Sakakibara, Y. Kato, B. Fåk, J. Ollivier, J. W. Lynn, T. Taniguchi, M. Wakita, and H. Kadowaki, Phys. Rev. Lett. **116**, 217201 (2016).
[25] Y.-D. Li and G. Chen, Phys. Rev. B **95**, 041106(R) (2017).
[26] E. Lhotel, S. Petit, S. Guitteny, O. Florea, M. Ciomaga Hatnean, C. Colin, E. Ressouche, M. R. Lees, and G. Balakrishnan, Phys. Rev. Lett. **115**, 197202 (2015).
[27] C. Mauws, A. M. Hallas, G. Sala, A. A. Aczel, P. M. Sarte, J. Gaudet, D. Ziat, J. A. Quilliam, J. A. Lussier, M. Bieringer, H. D. Zhou, A. Wildes, M. B. Stone, D. Abernathy, G. M. Luke, B. D. Gaulin, and C. R. Wiebe, Phys. Rev. B **98**, 100401(R) (2018).
[28] O. Benton, Phys. Rev. B **94**, 104430 (2016).
[29] S. Petit, E. Lhotel, B. Canals, M. C. Hatnean, J. Ollivier, H. Mutka, E. Ressouche, A. Wildes, M. Lees, and G. Balakrishnan, Nat. Phys. **12**, 746 (2016).
[30] R. Sibille, E. Lhotel, V. Pomjakushin, C. Baines, T. Fennell, and M. Kenzelmann, Phys. Rev. Lett. **115**, 097202 (2015).
[31] M. Hermele, M. P. A. Fisher, and L. Balents, Phys. Rev. B **69**, 064404 (2004).
[32] L. Savary and L. Balents, Phys. Rev. Lett. **108**, 037202 (2012).
[33] L. Savary and L. Balents, Phys. Rev. B **87**, 205130 (2013).
[34] O. Benton, O. Sikora, and N. Shannon, Phys. Rev. B **86**, 075154 (2012).

[35] H. Otobe, A. Nakamura, T. Yamashita, and K. Minato, J. Phys. Chem. Solids **66**, 329 (2005).
[36] See Supplemental Material at http://link.aps.org/supplemental/10.1103/PhysRevLett.122.187201 for details on experimental methods, crystal-field calculations and analysis of the neutron scattering experiments.
[37] J. B. Thomson, A. R. Armstrong, and P. G. Bruce, J. Solid State Chem. **148**, 56 (1999).
[38] J. B. Thomson, A. R. Armstrong, and P. G. Bruce, Chem. Commun. (Cambridge) 10 (**1996**) 1165.
[39] J. Gaudet, D. D. Maharaj, G. Sala, E. Kermarrec, K. A. Ross, H. A. Dabkowska, A. I. Kolesnikov, G. E. Granroth, and B. D. Gaulin, Phys. Rev. B **92**, 134420 (2015).
[40] A. J. Freeman and R. E. Watson, Phys. Rev. **127**, 2058 (1962).
[41] M. Blume, A. Freeman, and R. Watson, Phys. Rev. **134**, A320 (1964).
[42] J. H. VanVleck, *The Theory of Electronic and Magnetic Susceptibilities* (Oxford University Press, London, 1932).
[43] R. Azuah, L. Kneller, Y. Qiu, C. Brown, J. Copley, R. Dimeo, and P. Tregenna-Piggott, J. Res. Natl. Inst. Stand. Technol. **114**, 341 (2009).
[44] A. M. Hallas, J. Gaudet, M. N. Wilson, T. J. Munsie, A. A. Aczel, M. B. Stone, R. S. Freitas, A. M. Arevalo-Lopez, J. P. Attfield, M. Tachibana, C. R. Wiebe, G. M. Luke, and B. D. Gaulin, Phys. Rev. B **93**, 104405 (2016).
[45] G. E. Granroth, A. I. Kolesnikov, T. E. Sherline, J. P. Clancy, K. A. Ross, J. P. C. Ruff, B. D. Gaulin, and S. E. Nagler, J. Phys. Conf. Ser. **251**, 012058 (2010).
[46] J. Gaudet, A. M. Hallas, A. I. Kolesnikov, and B. D. Gaulin, Phys. Rev. B **97**, 024415 (2018).
[47] G. Sala, D. D. Maharaj, M. B. Stone, H. A. Dabkowska, and B. D. Gaulin, Phys. Rev. B **97**, 224409 (2018).
[48] J. Gaudet, A. M. Hallas, C. R. C. Buhariwalla, G. Sala, M. B. Stone, M. Tachibana, K. Baroudi, R. J. Cava, and B. D. Gaulin, Phys. Rev. B **98**, 014419 (2018).
[49] M. Ruminy, E. Pomjakushina, K. Iida, K. Kamazawa, D. T. Adroja, U. Stuhr, and T. Fennell, Phys. Rev. B **94**, 024430 (2016).
[50] K. Popa, R. Konings, F. Wastin, E. Colineau, N. Magnani, and P. Raison, J. Phys. Chem. Solids **69**, 70 (2008).
[51] B. C. den Hertog and M. J. P. Gingras, Phys. Rev. Lett. **84**, 3430 (2000).
[52] S. T. Bramwell, M. J. Harris, B. C. Den Hertog, M. J. P. Gingras, J. S. Gardner, D. F. McMorrow, A. R. Wildes, A. Cornelius, J. D. M. Champion, R. G. Melko, and T. Fennell, Phys. Rev. Lett. **87**, 047205 (2001).
[53] K. A. Ross, T. H. Proffen, H. A. Dabkowska, J. A. Quilliam, L. R. Yaraskavitch, J. B. Kycia, and B. D. Gaulin, Phys. Rev. B **86**, 174424 (2012).
[54] S. M. Koohpayeh, J.-J. Wen, B. A. Trump, C. L. Broholm, and T. M. McQueen, J. Cryst. Growth **402**, 291 (2014).
[55] K. Baroudi, B. D. Gaulin, S. H. Lapidus, J. Gaudet, and R. J. Cava, Phys. Rev. B **92**, 024110 (2015).
[56] K. E. Arpino, B. A. Trump, A. O. Scheie, T. M. McQueen, and S. M. Koohpayeh, Phys. Rev. B **95**, 094407 (2017).
[57] H. D. Zhou, C. R. Wiebe, J. A. Janik, L. Balicas, Y. J. Yo, Y. Qiu, J. R. D. Copley, and J. S. Gardner, Phys. Rev. Lett. **101**, 227204 (2008).
[58] K. Fritsch, K. A. Ross, Y. Qiu, J. R. D. Copley, T. Guidi, R. I. Bewley, H. A. Dabkowska, and B. D. Gaulin, Phys. Rev. B **87**, 094410 (2013).
[59] K. Kimura, S. Nakatsuji, J.-J. Wen, C. L. Broholm, M. B. Stone, E. Nishibori, and H. Sawa, Nat. Commun. **4**, 1934 (2013).
[60] R. Sibille, E. Lhotel, M. C. Hatnean, G. Balakrishnan, B. Fåk, N. Gauthier, T. Fennell, and M. Kenzelmann, Phys. Rev. B **94**, 024436 (2016).
[61] R. Sibille, N. Gauthier, H. Yan, M. C. Hatnean, J. Ollivier, B. Winn, U. Filges, G. Balakrishnan, M. Kenzelmann, N. Shannon, and T. Fennell, Nat. Phys. **14**, 711 (2018).
[62] L. Savary and L. Balents, Phys. Rev. Lett. **118**, 087203 (2017).
[63] J.-J. Wen, S. M. Koohpayeh, K. A. Ross, B. A. Trump, T. M. McQueen, K. Kimura, S. Nakatsuji, Y. Qiu, D. M. Pajerowski, J. R. D. Copley, and C. L. Broholm, Phys. Rev. Lett. **118**, 107206 (2017).
[64] O. Benton, Phys. Rev. Lett. **121**, 037203 (2018).
[65] H. R. Molavian, M. J. P. Gingras, and B. Canals, Phys. Rev. Lett. **98**, 157204 (2007).
[66] S. Petit, E. Lhotel, S. Guitteny, O. Florea, J. Robert, P. Bonville, I. Mirebeau, J. Ollivier, H. Mutka, E. Ressouche, C. Decorse, M. Ciomaga Hatnean, and G. Balakrishnan, Phys. Rev. B **94**, 165153 (2016).
[67] B. Gao *et al.*, arXiv:1901.10092.